Available online at www.sciencedirect.com
SCIENCE DIRECT®
Journal of Nuclear Materials 341 (2005) 19–24
journal of nuclear materials
www.elsevier.com/locate/jnucmat

Phase relations and linear thermal expansion of cubic solid solutions in the $Th_{1-x}M_xO_{2-x/2}$ (M = Eu, Gd, Dy) systems

M.D. Mathews, B.R. Ambekar, A.K. Tyagi *

Applied Chemistry Division, Bhabha Atomic Research Centre, Mumbai 400 085, India

Received 23 July 2004; accepted 17 December 2004

Abstract

Cell parameters and linear thermal expansion studies of the Th–M oxide systems with general compositions $Th_{1-x}M_xO_{2-x/2}$ ($M = Eu^{3+}$, Gd^{3+} and Dy^{3+}, $0.0 \leqslant x \leqslant 1.0$) are reported. The XRD patterns of each product were refined to specify the solid solubility limits of $MO_{1.5}$ in the ThO_2 lattice. The upper solid solubility limits of $EuO_{1.5}$, $GdO_{1.5}$ and $DyO_{1.5}$ in the ThO_2 lattice under conditions of slow cooling from 1673 K are represented as $Th_{0.50}Eu_{0.50}O_{1.75}$, $Th_{0.60}Gd_{0.40}O_{1.80}$ and $Th_{0.85}Dy_{0.15}O_{1.925}$, respectively. The linear thermal expansion (293–1123 K) of $MO_{1.5}$ and their single-phase solid solutions with thoria were investigated by dilatometery. The average linear thermal expansion coefficients ($\bar{\alpha}$) of the compounds decrease on going from $EuO_{1.5}$ to $DyO_{1.5}$. The values of $\bar{\alpha}$ for $EuO_{1.5}$, $GdO_{1.5}$ and $DyO_{1.5}$ containing solid solutions showed a downward trend as a function of the dopant concentration. The linear thermal expansion (293–1473 K) of the solid solutions investigated by high-temperature XRD also showed a similar trend.

1. Introduction

In nuclear reactors involving UO_2 and $(U,Th)O_2$ fuels, two types of solid fission products are found viz. metallic and non-metallic inclusions [1–3]. Among the non-metallic solid fission product compounds, the rare-earth oxides, Ln_2O_3 (Ln = La, Ce, Y, Nd, Sm, Eu and Gd), ZrO_2 and alkaline-earth oxides MO (M = Sr and Ba) are the major inclusions. These fission products are known to form solid solutions with UO_2, while mainly rare-earth oxides are known to be soluble in the ThO_2 and $(U,Th)O_2$ lattice [4–6].

Thorium has attracted a considerable attention in the recent past as it is expected to play an important role in the third stage of the Indian Nuclear Power generation [7], In this context, we have been investigating various thorium-based mixed oxide systems. One of the major activities is on the thermal expansion behaviour of different thoria-based systems having relevance to the proposed thorium oxide-based nuclear reactors. Thermal expansion is an important parameter governing the performance of a nuclear fuel pin assembly. As a part of this research activity, the thermal expansion behaviour of ThO_2 containing 2 wt% UO_2 has been investigated by high-temperature X-ray diffractometry [8]. The preparation and thermal expansion studies of $BaThO_3$ and $SrThO_3$ were also reported [9].

* Corresponding author. Tel.: +91 22 2559 5330; fax: +91 22 2550 5151.
E-mail address: aktyagi@magnum.barc.ernet.in (A.K. Tyagi).

0022-3115/$ - see front matter © 2005 Elsevier B.V. All rights reserved.
doi:10.1016/j.jnucmat.2004.12.007

Doped thoria is an important material in view of its potential applications as a solid electrolyte for its use in oxygen concentration cells. There are little data on the thermodynamic and thermophysical properties of mixed oxides based on thoria compared to those of urania. There are a few reports on the solubility of Nd_2O_3, Eu_2O_3, Gd_2O_3 and Dy_2O_3 in the ThO_2 lattice under long-annealed in situ and quenched conditions. Among them, the phase relations in the ThO_2–$NdO_{1.5}$ and ThO_2–$GdO_{1.5}$ systems have been reported way back in 1954 by Brauer et al. [10]. They reported a solubility of about 50 mol% of both $NdO_{1.5}$ and $GdO_{1.5}$ at 1673 K in the ThO_2 lattice. However, according to Sibieude et al. [11] only 35 mol% $NdO_{1.5}$ and 20 mol% $GdO_{1.5}$ are soluble in ThO_2 at 1673 K and their solubilities increased to 40 and 50 mol%, respectively, at 2473 K. The sub-solidus phase relation in the ThO_2–$GdO_{1.5}$ system as investigated by Diness et al. [5] showed that the solubility of $GdO_{1.5}$ in ThO_2 increased from 30 mol% at 1673 K to 45 mol% at 2273 K. The effect of temperature on the solubility of $DyO_{1.5}$ [10] and of $EuO_{1.5}$ [12] in ThO_2 has been also reported. Accordingly at 1673 K, about 15 mol% $DyO_{1.5}$ were found to be soluble in ThO_2 which increased substantially to 50 mol% at 2473 K. According to Gingerich et al. [12] the solubility of $EuO_{1.5}$ in ThO_2 increased from 36 mol% at 1473 K to 47 mol% at 1673 K. They also observed that the cell parameters of the solid solutions decreased systematically with increasing $EuO_{1.5}$ content. The decrease in cell parameter as well as of the thermal diffusivity and thermal conductivity of $Th_{1-x}Eu_xO_{2-x/2}$ ($0.0 < x < 0.30$) solid solutions with the increase in $EuO_{1.5}$ content have also been reported by Murti et al. [6]. Since all of these phase relations were established in static air, the effect of oxygen partial pressure on solubility limits can be ignored.

There are little data on the phase relations in the thoria-rare-earth oxide systems under slow-cooled conditions and also on the thermal expansion behaviour of the solid solutions formed in such systems. Our recent studies [13] on the phase relations and thermal expansion behaviour of the thoria–neodymia system showed that, under conditions of slow cooling from 1673 K, 50 mol% of $NdO_{1.5}$ is soluble in ThO_2 while retaining the fluorite lattice, and that the coefficients of the average linear thermal expansion of the single-phase solid solutions increased with increasing $NdO_{1.5}$ content.

In this paper, we report on the phase relations in the $Th_{1-x}M_xO_{2-x/2}$ ($M = Eu^{3+}$, Gd^{3+} and Dy^{3+}, $0.0 \leqslant x \leqslant 1.0$) systems under slow-cooled conditions and on the thermal expansion behaviour of the single-phase solid solutions formed in these systems. The rare-earth ions have been chosen as guest ions because they are the major fission products in nuclear fuels. They are also of interest in reactor technology as neutron absorbers and burn-up monitors, and it is desired to know their chemical states in the nuclear fuel host lattice. Thermal expansion is an important property, which governs the performance of the nuclear fuel pin assembly. Therefore, the investigations in these systems were undertaken.

2. Experimental

The AR grade rare-earth oxide Eu_2O_3, Gd_2O_3 and Dy_2O_3 and ThO_2 (99.9%, obtained from Indian rare-earths), were first dried by heating at 1173 K for overnight. Appropriate mixtures to give the nominal compositions $Th_{1-x}M_xO_{2-x/2}$ were prepared by an intimate mixing of the starting materials and were pressed into 8 mm pellets and heated at 1473 K for 36 h, followed by one more heating after regrinding at 1573 K again for 36 h. Each product was once again ground well, pelletized and heated at 1673 K for 48 h followed by slow cooling to room temperature at the rate of 2 K/min. All the heatings were done in static air. The XRD patterns were recorded by X-ray difrractometry (Philips Model PW 1710) with Ni-filtered Cu-Kα radiation. Silicon was used as an external standard. The XRD patterns were analyzed by comparing with the reported ones. In order to determine the solubility limits, the lattice parameters were refined by a least-squares method.

The thermal expansion studies were carried out on selected single-phase compositions within the solubility limits of $MO_{1.5}$ in the ThO_2 lattice as well as of the high-temperature forms of $EuO_{1.5}$ and $GdO_{1.5}$ (monoclinic) and ambient temperature form of $DyO_{1.5}$ (cubic). For the thermal expansion measurements by dilatometry, samples were pressed and sintered to about 10 mm diameter and 10 mm height pellets with densities about 80% th. d. The linear thermal expansion was measured in air as a function of temperature up to 1123 K on a LKB 3185 fused quartz thermodilatometer. Due to the hygroscopic nature of the samples, the pellets were mounted in the dilatometer immediately after taking out of the furnace used for the preparation of the samples. High-temperature X-ray powder diffraction (HT-XRD) studies were carried out using a Philips Xpert Pro Unit having an Anton Paar high-temperature attachment. The XRD patterns were recorded in the range $2\theta = 10°$ to $90°$ between 293 and 1473 K in a step of 200 K under vacuum of the order of $3 \cdot 10^{-8}$ bar. The unit cell parameters were determined using a least-squares refinement program. The average quasi-isotropic linear thermal expansion ($\bar{\alpha}_i$) were also evaluated in each case. It may be noted that since the thermal expansion measurements using HT-XRD were performed on polycrystalline cubic samples, it is presumed that a quasi-isotropic expansion behaviour is exhibited by these samples.

3. Results and discussion

3.1. Cell parameters

The phase identification and cell parameters at room temperature are given in Table 1. As can be seen, the fluorite-type structure is retained up to the compositions of $Th_{0.50}Eu_{0.50}O_{1.75}$, $Th_{0.60}Gd_{0.40}O_{1.80}$ and $Th_{0.85}Dy_{0.15}O_{1.925}$ in the respective systems. It implies that the solubility of $EuO_{1.5}$, $GdO_{1.5}$ and $DyO_{1.5}$ in the ThO_2 lattice, under the preparation conditions used in the present study, is 50, 40 and 15 mol%, respectively. The solubility behavior of Eu^{3+}, Gd^{3+} and Dy^{3+} in the lattice of ThO_2 can be attributed to the ionic radii difference between host and guest ions. The ionic radii of Th^{4+}, Eu^{3+}, Gd^{3+} and Dy^{3+} are 105 pm, 98 pm, 97 pm and 94 pm, respectively, in eightfold coordination [14] As the difference between ionic radii of host and guest ions increases, the solubility limit decreases and the minimum solubility is with the system of the largest difference in ionic radii of host and guest ions i.e., Th^{4+}–Dy^{3+} combination. The present results reveal that the solubility limits of Eu^{3+}, Gd^{3+} and Dy^{3+} in the ThO_2 lattice under long-annealed and quenched-conditions as reported by Brauer et al. [10] and Gingerich et al. [12] and under short-annealed and slow-cooled conditions of present investigations do not differ much. Beyond the compositions of $Th_{0.45}Eu_{0.55}O_{1.725}$, $Th_{0.55}Gd_{0.45}O_{1.775}$ and $Th_{0.80}Dy_{0.20}O_{1.90}$, additional peaks started to appear which could be identified due to the respective rare-earth oxides (the monoclinic modification of $EuO_{1.5}$ and $GdO_{1.5}$, the cubic modification of $DyO_{1.5}$). These additional peaks subsequently grew in intensity with the increase of the respective $MO_{1.5}$ concentration. Some typical XRD patterns pertaining to ThO_2–$DyO_{1.5}$ system are given in Fig. 1. No ordered phases were identified in these systems, as the large difference in host and guest ionic radii is the main driving force for ordering, contrary to the comparatively small difference in ionic radii in the present systems.

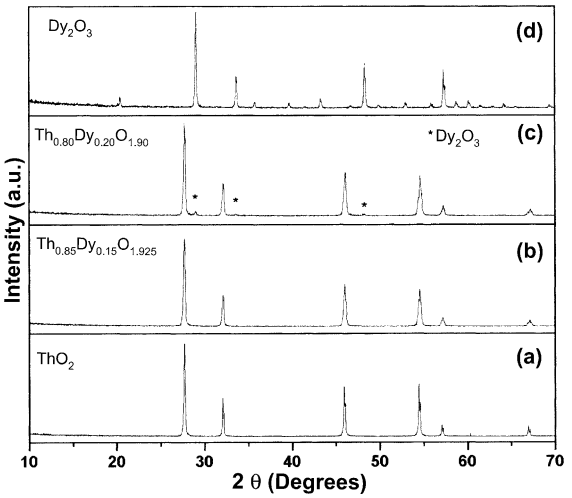

Fig. 1. Room temperature XRD patterns of (a) ThO_2, (b) $Th_{0.85}Dy_{0.15}O_{1.925}$, (c) $Th_{0.80}Dy_{0.20}O_{1.90}$, (d) Dy_2O_3.

The cubic lattice parameters of all single-phase products show a gradual decrease with increasing content of the dopants. The difference in ionic radii of guest and host ions is well reflected in the trend of the cell parameters of the solid solutions in the respective systems.

3.2. Linear thermal expansion

The linear thermal expansion study on the title solid solutions as well as the monoclinic modification of Eu_2O_3 and Gd_2O_3 and the cubic modification of Dy_2O_3 was carried out by dilatometry from 293 to 1123 K. Typical plots of the linear thermal expansion (%) versus temperature of $Th_{0.90}M_{0.10}O_{1.95}$ and of M_2O_3 (M = Eu^{3+}, Gd^{3+} and Dy^{3+}) are shown in Figs. 2 and 3, respectively. The dilatometric result of ThO_2 as reported earlier [15] is also shown in Fig. 3 for comparison. The observed

Table 1
Room temperature lattice parameters of fluorite type solid solutions in the $Th_{1-x}M_xO_{2-x/2}$ (M = Eu^{3+}, Gd^{3+} and Dy^{3+}) systems

Sr. no.	Nominal composition	$MO_{1.50}$ (mol%)	Cubic lattice parameter a (nm)		
			Eu^{3+}	Gd^{3+}	Dy^{3+}
1	$Th_{1.0}M_{0.0}O_{2.0}$	0.00	0.5600 (1)	0.5600 (1)	0.5600 (1)
2	$Th_{0.90}M_{0.10}O_{1.95}$	10.00	0.5585 (1)	0.5585 (1)	0.5578 (1)
3	$Th_{0.85}M_{0.15}O_{1.925}$	15.00	–	–	0.5568 (1)
4	$Th_{0.80}M_{0.20}O_{1.90}$	20.00	0.5581 (2)	0.5579 (1)	*
5	$Th_{0.70}M_{0.30}O_{1.85}$	30.00	0.5573 (1)	0.5567 (2)	
6	$Th_{0.60}M_{0.40}O_{1.80}$	40.00	0.5566 (1)	0.5565 (1)	
7	$Th_{0.50}M_{0.50}O_{1.75}$	50.00	0.5563 (1)	*	
8	$Th_{0.45}M_{0.55}O_{1.725}$	55.00	*		

* Two phase (fluorite-type phase and the corresponding $REO_{1.5}$).

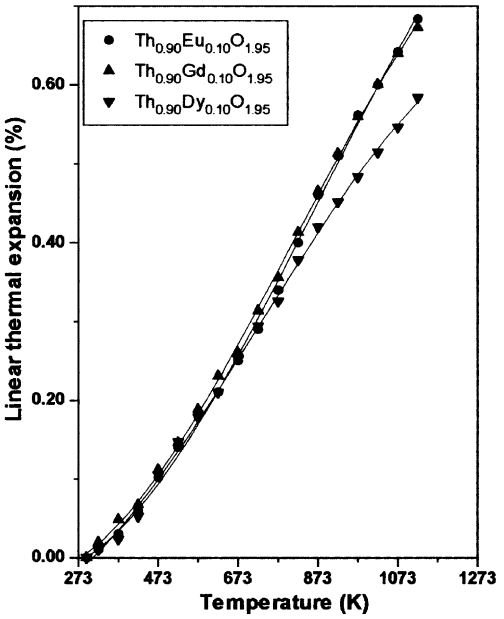

Fig. 2. Linear thermal expansion (%) of a few representative solid solutions as a function of temperature.

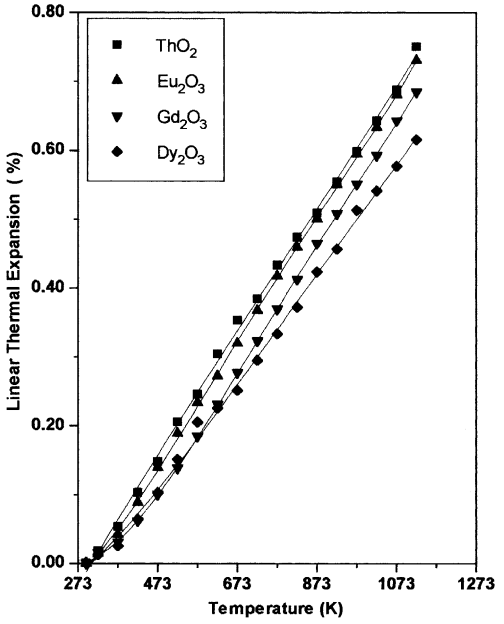

Fig. 3. Linear thermal expansion (%) of starting materials as a function of temperature.

linear thermal expansion (%) was fitted as a function of temperature using a general polynomial regression as given below and the fitting parameters are given in Table 2 (T in K and $T_{ref} = 293$ K)

$$100 \cdot \Delta l/l_o = a + bT + cT^2 + dT^3 + eT^4.$$

The average linear thermal expansion coefficients $\bar{\alpha}$ (293–1123 K) of all the compositions are given in Table 3. It is observed that the $\bar{\alpha}$ values of the solid solutions in all the three systems decrease progressively with the increase of the dopant content.

The lattice parameters of the solid solutions at different temperatures are given in Table 4 and a typical plot of the variation of cell parameters of $Th_{0.90}M_{0.10}O_{1.95}$ (M = Eu, Gd and Dy) as a function of temperature is shown in Fig. 4. The cell parameters of the solid solutions showed a nearly linear increase with the increase in temperature.

The average quasi-isotropic linear thermal expansion coefficients ($\bar{\alpha}_i$) of the solid solutions as evaluated from the cell parameters in the temperature ranges of 293–1123 K, so as to compare with dilatometry data in same temperature range, and 293–1473 K are also given in Table 5. The values of $\bar{\alpha}$ and $\bar{\alpha}_i$ of each solid solution of the systems are found to be well comparable with one another (Tables 3 and 5).

It is also evident from the Table 5 that the coefficients of average linear thermal expansion of the compounds decrease on going from Eu_2O_3 to Dy_2O_3 in the temperature range of investigation. The observed trend of thermal expansion of the compounds appears to be more related to the ionic radii of the cations of the compounds, i.e. the larger the ionic radii of the cations, the higher the thermal expansion. Another reason could be that the degree of covalent character increases on going from Eu–O bond to Gd–O bond to Dy–O bond, which also might be responsible for a downward trend in thermal expansion coefficients in this order. Also, in general it is observed that if the compounds with higher structural symmetry show higher thermal expansion compared to that with lower symmetry. The thermal expansion characteristics of the compounds of Eu_2O_3, Gd_2O_3 and Dy_2O_3 seem to contribute significantly to the thermal expansion behaviour of the solid solutions which they form with thoria. Thus in general, the linear and quasi-isotropic linear thermal expansion coefficients of $Th_{1-x}M_xO_{2-x/2}$ solid solutions with the same compositional value of 'x' also show a decreasing trend on going from Eu^{3+} to Dy^{3+}. The linear thermal expansion of the solid solutions of other systems decrease progressively on increasing content of the respective dopants. The decrease in linear thermal expansion coefficients of these solid solutions on increasing the content of the dopants can also be explained based on the low values of thermal expansion coefficients of Eu_2O_3, Gd_2O_3 and Dy_2O_3 compared to that of ThO_2 (Tables 2 and 4). Another reason could be that as the Eu, Gd and Dy contents increase, defect concentration (oxygen vacancy) also increases which can mask thermal expansion to some extent.

Table 2
The fitting parameters of the linear thermal expansion (%) as a function of temperature ($100 \cdot \Delta l/l_o = a + bT + cT^2 + dT^3 + eT^4$), 293–1123 K

Composition	a	b	c	d	e
ThO_2	+0.12350	−0.00193	$+7.03017 \times 10^{-6}$	-7.17758×10^{-9}	$+2.57736 \times 10^{-12}$
$Th_{0.90}Eu_{0.10}O_{1.95}$	−0.23369	+0.00128	-2.58844×10^{-6}	$+3.66612 \times 10^{-9}$	-1.53903×10^{-12}
$Th_{0.80}Eu_{0.20}O_{1.90}$	−0.16721	$+6.28825 \times 10^{-4}$	-4.30937×10^{-7}	$+9.20422 \times 10^{-10}$	-4.33069×10^{-13}
$Th_{0.70}Eu_{0.30}O_{1.85}$	+0.08619	−0.00125	$+4.34492 \times 10^{-6}$	-4.1038×10^{-9}	$+1.39466 \times 10^{-12}$
$Th_{0.60}Eu_{0.40}O_{1.80}$	−0.05463	-4.58214×10^{-4}	$+3.12005 \times 10^{-6}$	-3.54788×10^{-9}	$+1.39437 \times 10^{-12}$
$Th_{0.50}Eu_{0.50}O_{1.75}$	−0.09015	-1.90442×10^{-4}	$+2.44604 \times 10^{-6}$	-2.8867×10^{-9}	$+1.16297 \times 10^{-12}$
$Th_{0.90}Gd_{0.10}O_{1.95}$	−0.20891	$+9.22334 \times 10^{-4}$	-1.60980×10^{-6}	$+2.6946 \times 10^{-9}$	$+1.23343 \times 10^{-12}$
$Th_{0.80}Gd_{0.20}O_{1.90}$	−0.03439	-3.40181×10^{-4}	$+1.87541 \times 10^{-6}$	-1.11746×10^{-9}	$+1.57787 \times 10^{-13}$
$Th_{0.70}Gd_{0.30}O_{1.85}$	−0.19722	$+8.83604 \times 10^{-4}$	-1.24355×10^{-6}	$+2.08902 \times 10^{-9}$	-1.01243×10^{-12}
$Th_{0.60}Gd_{0.40}O_{1.80}$	+0.00722	-5.82169×10^{-4}	$+2.49267 \times 10^{-6}$	-2.23026×10^{-9}	$+7.40232 \times 10^{-12}$
$Th_{0.90}Dy_{0.10}O_{1.95}$	+0.07480	−0.00118	$+4.17856 \times 10^{-6}$	-3.87536×10^{-9}	$+1.31581 \times 10^{-12}$
$Th_{0.85}Dy_{0.15}O_{1.925}$	+0.10207	−0.00126	$+3.98693 \times 10^{-6}$	-3.26191×10^{-9}	$+9.34238 \times 10^{-13}$
Eu_2O_3	+0.02049	-9.94114×10^{-4}	$+4.17846 \times 10^{-6}$	-3.87301×10^{-9}	$+1.28679 \times 10^{-12}$
Gd_2O_3	+0.20259	−0.00193	$+5.41175 \times 10^{-4}$	-4.42989×10^{-9}	$+1.32076 \times 10^{-12}$
Dy_2O_3	−0.06714	-1.55886×10^{-4}	$+1.647888 \times 10^{-6}$	-1.23927×10^{-9}	$+3.42031 \times 10^{-13}$

Table 3
Coefficients of average linear thermal expansion ($\bar{\alpha}$) by dilatometry of $Th_{1-x}M_xO_{2-x/2}$ solid solutions, 293–1123 K

Sr. no.	Nominal composition	$\bar{\alpha} \pm 0.30$ (10^6 K^{-1})[a]		
		M = Eu^{3+}	Gd^{3+}	Dy^{3+}
1	$Th_{1.0}M_{0.0}O_2$	9.04	9.04	9.04
2	$Th_{0.90}M_{0.10}O_{1.95}$	8.24	8.10	7.48
3	$Th_{0.85}M_{0.15}O_{1.925}$	–	–	7.04
4	$Th_{0.80}M_{0.20}O_{1.90}$	7.30	7.53	–
5	$Th_{0.70}M_{0.30}O_{1.85}$	6.80	7.03	–
6	$Th_{0.60}M_{0.40}O_{1.80}$	6.57	6.24	–
7	$Th_{0.50}M_{0.50}O_{1.75}$	6.46	–	–
8	$Th_{0.0}M_{0.10}O_{1.5}$	8.80	8.25	7.41

[a] $\bar{\alpha}_i = 100 \cdot \Delta l/l_{293}(T - 293)$. Δl is the increase in length of the sample on increasing the temperature from 293 to 'T' K, l_{293} is the length of the sample at 293 K.

Table 4
Lattice parameters of the fluorite-type solid solutions in $Th_{1-x},M_xO_{2-x/2}$ systems at different temperatures

Sr. no.	Solid solution	Lattice parameters a (nm)						
		293 K	473 K	673 K	873 K	1123 K	1273 K	1473 K
1	$Th_{0.90}Eu_{0.1}O_{1.95}$	0.5585	0.5593	0.5605	0.5614	0.5627	0.5636	0.5647
2	$Th_{0.80}Eu_{0.2}O_{1.90}$	0.5581	0.5586	0.5591	0.5601	0.5619	0.5628	0.5642
3	$Th_{0.70}Eu_{0.30}O_{1.85}$	0.5573	0.5580	0.5585	0.5594	0.5609	0.5619	0.5632
4	$Th_{0.60}Eu_{0.40}O_{1.80}$	0.5566	0.5676	0.5579	0.5587	0.5599	0.5609	0.5623
5	$Th_{0.50}Gd_{0.5}O_{1.75}$	0.5563	0.5568	0.5571	0.5583	0.5595	0.5604	0.5617
6	$Th_{0.90}Gd_{0.10}O_{1.95}$	0.5585	0.5593	0.5604	0.5614	0.5626	0.5636	0.5647
7	$Th_{0.80}Gd_{0.20}O_{1.90}$	0.5579	0.5586	0.5592	0.5602	0.5617	0.5628	0.5639
8	$Th_{0.70}Gd_{0.30}O_{1.85}$	0.5567	0.5574	0.5577	0.5588	0.5601	0.5612	0.5625
9	$Th_{0.60}Gd_{0.40}O_{1.80}$	0.5567	0.5574	0.5577	0.5590	0.5599	0.5611	0.5624
10	$Th_{0.90}Dy_{0.10}O_{1.95}$	0.5578	0.5585	0.5593	0.5603	0.5617	0.5626	0.5639
11	$Th_{0.850}Dy_{0.15}O_{1.925}$	0.5568	0.5575	0.5581	0.5592	0.5606	0.5615	0.5628

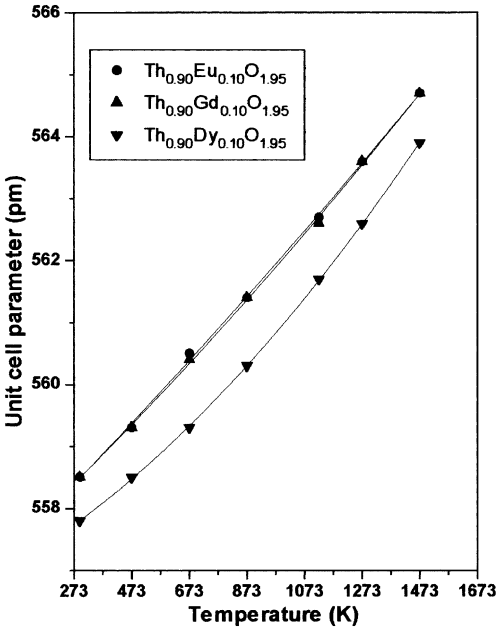

Fig. 4. Unit cell parameters of a few representative solid solutions as a function of temperature.

Table 5
Coefficients of average linear thermal expansion ($\bar{\alpha}_i$) by X-ray diffractometry of $Th_{1-x}M_xO_{2-x/2}$ (M = Eu^3, Gd^{3+} and Dy^{3+}) solid solutions

Sr. no.	Nominal composition	$\bar{\alpha}_i(10^6\ K^{-1})$ (293–1123 K)[a] $\bar{\alpha}_i(10^6\ K^{-1})$ (293–1473 K)[a,*]		
		Eu^{3+}	Gd^{3+}	Dy^{3+}
1	$Th_{1.0}M_{0.0}O_2$	9.13	9.13	9.13
		9.55*	9.55*	9.55*
2	$Th_{0.9}M_{0.10}O_{1.95}$	9.06	8.84	8.42
		9.41*	9.41*	9.27*
3	$Th_{0.85}M_{0.15}O_{1.925}$	–	–	8.22
				9.13*
4	$Th_{0.80}M_{0.20}O_{1.90}$	8.20	8.20	–
		9.26*	9.11*	–
5	$Th_{0.7}M_{0.30}O_{1.85}$	7.57	7.57	–
		8.81*	8.83*	–
6	$Th_{0.60}M_{0.40}O_{1.80}$	7.14	6.92	–
		8.68*	8.68*	–
7	$Th_{0.50}M_{0.50}O_{1.75}$	6.93	–	–
		8.22*	–	–

[a] $\bar{\alpha}_i = 100 \cdot \Delta a/a_{293}(T - 293)$. Δa is the increase in cell parameter on increasing the temperature from 293 to 'T' K, a_{293} is the cell parameter at 293 K.

4. Conclusions

The phase relation studies have been carried out in the $Th_{1-x}M_xO_{2-x/2}$ (M = Eu, Gd and Dy) systems. The detailed XRD analysis of the phases was used to delineate the phase boundaries in the systems. There are two distinct regions in the systems viz. a solid solution of $MO_{1.5}$ in ThO_2, which are identified as cubic fluorite and a biphasic region of ThO_2 type and $MO_{1.5}$ type phases. The linear thermal expansion of $MO_{1.5}$ compounds as well as $MO_{1.5}$ doped single-phase solid solutions also have been carried out. The values of the linear thermal expansion coefficients of the solid solutions are found to decrease on going from $EuO_{1.5}$ to $DyO_{1.5}$. These observations would be useful in knowing the chemical state of these rare-earths in ThO_2-based nuclear fuels at different burn-ups and their influence on the thermal expansion.

Acknowledgement

We thank Dr N.M. Gupta, Head, Applied Chemistry Division for his keen interest and encouragement to this work.

References

[1] H. Kleykamp, J. Nucl. Mater. 131 (1985) 221.
[2] E.H.P. Cordfunke, R.J.M. Konings, J. Nucl. Mater. 152 (1988) 301.
[3] C.E. Johnson, I. Johnson, P.E. Blackburn, C.E. Crouthamel, Reactor Technol. 15 (1972–1973) 303.
[4] K. Une, M. Oguma, J. Nucl. Mater. 84 (1979) 26.
[5] A.M. Diness, B. Rustam, J. Mater. Sci. 4 (1969) 613.
[6] P.S. Murti, C.K. Mathews, High Temp. High Press. 22 (1990) 379.
[7] R. Chidambaram, in: M. Srinivasan, I. Kimura (Eds.), Proc. Indo-Japan Seminar on Thoria Utilization, Bombay, India, Indian Nuclear Society and Atomic Energy Society of Japan, December 1990, p. 7.
[8] A.K. Tyagi, M.D. Mathews, J. Nucl. Mater. 278 (2000) 123.
[9] R.D. Purohit, A.K. Tyagi, M.D. Mathews, S. Saha, J. Nucl. Mater. 280 (2000) 51.
[10] G. Brauer, H. Gradinger, Z. Anorg. Allg. Chem. 276 (1954) 209.
[11] F. Sibieude, M. Foex, J. Nucl. Mater. 56 (1975) 229.
[12] K. Gingerich, G. Brauer, Z. Anorg. Allg. Chem. 324 (1963) 48.
[13] M.D. Mathews, B.R. Ambekar, A.K. Tyagi, J. Alloys Compd., in press.
[14] VCH Periodic Table of Elements, 1995, Compiled by Fluck & Heumann.
[15] M.D. Mathews, B.R. Ambekar, A.K. Tyagi, J. Nucl. Mater. 288 (2001) 83.